THE UNIVERSITY OF MICHIGAN

INDUSTRY PROGRAM OF THE COLLEGE OF ENGINEERING

TRANSIENT PHENOMENA ASSOCIATED WITH THE PRESSURIZED-DISCHARGE OF A CRYOGENIC LIQUID FROM A CLOSED VESSEL

J. A. Clark

G. J. Van Wylen

S. K. Fenster

October, 1959

IP-388

ACKNOWLEDGEMENT

This work was supported by the United States Army Ballistic Missile Agency, Redstone Arsenal, Huntsville, Alabama. The assistance of Mr. H. G. Paul and Mr. R. R. Head of ABMA is gratefully acknowledged. Mr. W. A. Warren, formerly a graduate student in the Department of Mechanical Engineering and now with the Linde Company, Buffalo, New York, contributed significantly to the research work.

Nomenclature

A	annular area of vessel wall
a	$k/\rho\ c_p$, thermal diffusivity of wall
a_1	$1/2\ (m + \sqrt{m^2 + 4\ p_1})$
a_2	$1/2\ (\sqrt{m^2 + 4\ p_2} - m)$
a_L	$1/2\ (m + \sqrt{m^2 + 4\ p_L})$
a_g	$1/2\ (\sqrt{m^2 + 4\ p_g} - m)$
C	mean circumference of vessel
c_p	specific heat of wall material
$\bar{h}_a, \bar{h}_g, \bar{h}_L$	coefficients of heat transfer for ambient, gas, and liquid, respectively
h	enthalpy
k	thermal conductivity of wall material
L	$\dfrac{\bar{h}_g\ C(t_{g\infty} - t_i)}{kA}$
m	$\dfrac{\rho\ VA\ c_p}{kA} = \dfrac{\rho\ V\ c_p}{k} = \dfrac{V}{a}$
p_2	$\dfrac{\bar{h}_a C + \bar{h}_g C}{kA}$
p_1	$\dfrac{\bar{h}_a C + \bar{h}_L C}{kA}$
p_L	$\dfrac{\bar{h}_L C}{kA}$
p_g	$\dfrac{\bar{h}_g C}{kA}$
q_2	$\dfrac{\bar{h}_a C t_a + \bar{h}_g C t_{g\infty}}{kA}$
q_1	$\dfrac{\bar{h}_a C t_a + \bar{h}_L C t_L}{kA}$

Nomenclature (Cont'd)

t — temperature of vessel wall

t^* — temperature of vessel wall at $x = 0$ (liquid-gas interface)

t_2 — temperature of vessel wall at $x = \infty$ for heat transfer with ambient:

$$t_2 = \frac{\bar{h}_a t_a + \bar{h}_g t_{g\infty}}{\bar{h}_a + \bar{h}_g}$$

t_1 — temperature of vessel wall at $x = -\infty$ for heat transfer with ambient:

$$t_1 = \frac{\bar{h}_a t_a + \bar{h}_L t_L}{\bar{h}_a + \bar{h}_L}$$

t_2' — temperature of vessel wall at $x = \infty$ for constant input heat flux:

$$t_2' = \frac{(q/A)w}{\bar{h}_g} + t_{g\infty}$$

t_1' — temperature of vessel wall at $x = -\infty$ for constant input heat flux:

$$t_1' = \frac{(q/A)w}{\bar{h}_L} + t_L$$

t_g — temperature of gas

t_i — temperature of gas at $x = 0$ (equal to saturation temperature at 50 psia)

$t_{g\infty}$ — temperature of gas at $x = \infty$

t_L — temperature of liquid

V — velocity of vessel wall (equal to liquid-vapor interfacial velocity)

x_t — location of thermocouple

x_i — location of liquid-gas interface

X — $x_t - x_i$

ρ — density of vessel wall

γ — exponent describing vapor temperature distribution, Equation (4)

θ — time

INTRODUCTION

The work reported in this paper was undertaken as part of a general research program directed at a study of the heat-mass transfer processes associated with the pressurized-discharge of a cryogenic liquid from a closed vessel. The fluids used were liquid nitrogen pressurized with gaseous nitrogen at approximately 50 psia and inlet temperatures ranging from -299°F to +111°F. Some of the initial results were given in Reference (1). Other work is reported in a companion paper.[2]

This paper is concerned with an analysis and experimental measurement of the thermal response of the vessel wall during the process of emptying for the cases of (i) and uninsulated vessel exchanging heat with the ambient and (ii) a vessel having a constant input heat flux imposed on its exterior surface. Also considered is the condensation of pressurizing gas on the liquid interface. A sketch of the experimental test vessel is shown in Figure 1.

The results of this study have application in the thermal analysis of pressurize-discharge processes where consideration is to be given to wall and liquid temperature transients, especially in the vicinity of the liquid-gas interface.

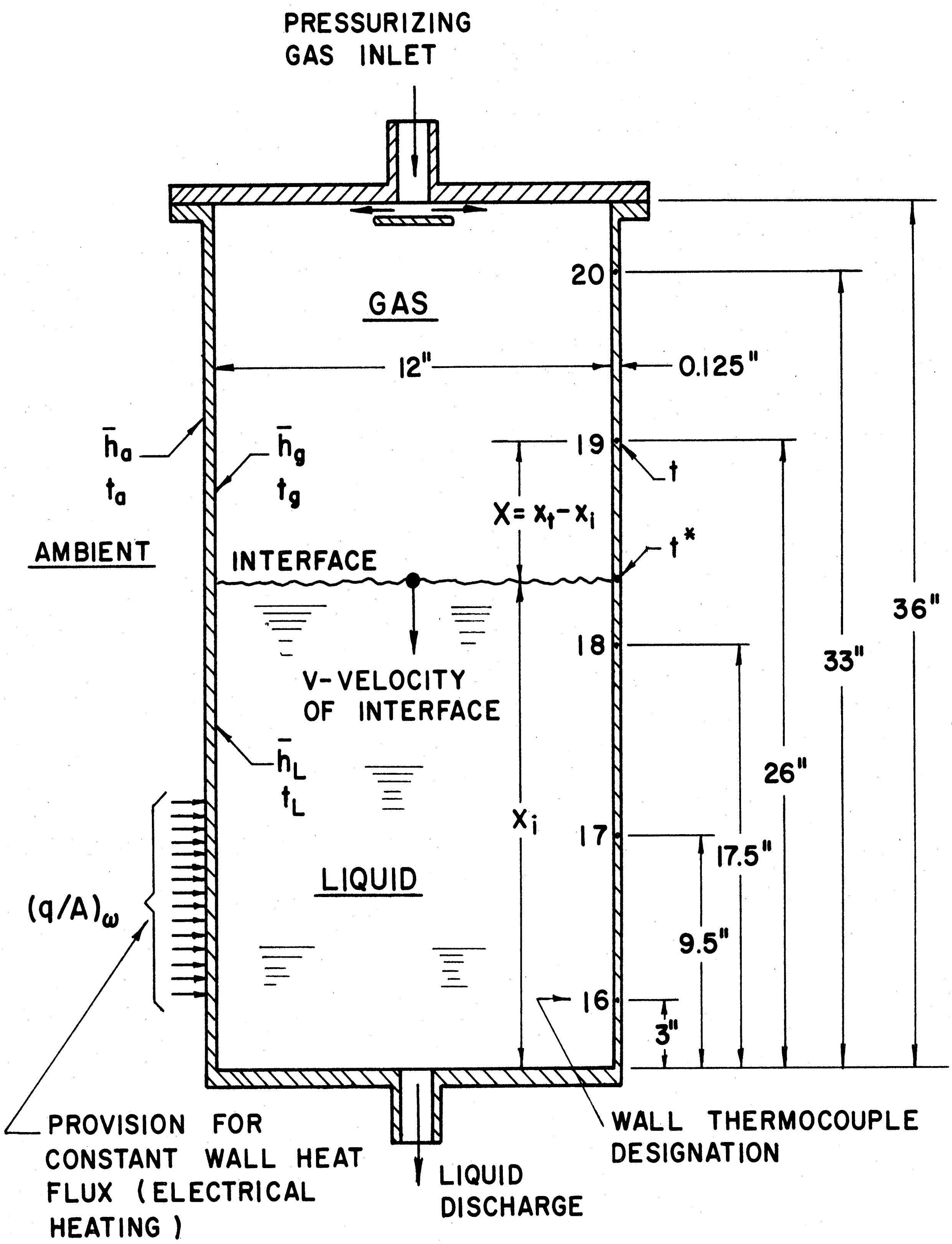

FIG. 1 EXPERIMENTAL TEST VESSEL (5052 ALUMINUM)

Analysis of Wall Temperature Transients

The system analyzed is shown in Figure 1 and attention is directed to the response of the temperature of the vessel wall.* The vessel initially is nearly filled with liquid. Subsequent to the filling a pressurizing gas is pumped into the gas space and the system is pressurized to approximately 50 psia. A discharge process is then begun with the pressurizing gas driving the liquid out the bottom of the tank. During this process the wall is exposed simultaneously to three media, the liquid, the pressurizing gas and the ambient. The ambient consists of a high temperature gas or a constant input heat flux. At its inside surface those portions of the wall which initially are covered with liquid are brought into contact with the pressurizing gas at the passage of the liquid-vapor interface during discharge. The wall also experiences an axial heat conduction.

Because the three media in contact with the wall and hence the wall itself are non-uniform in temperature all portions of the wall undergo thermal transients. The movement of the liquid-vapor interface further complicates the nature of this transients by introducing a timewise variable boundary condition on the inside surface.

The analysis which follows assumes that where the wall exchanges heat with its environment it does so either through a heat transfer

---

* It is assumed that the wall temperature varies with time only along its axial direction and is uniform throughout its thickness at any axial location. This condition is very closely obtained in any solid undergoing transient heat conduction when the Biot Number, $\bar{h}$(volume or solid/area wetted)/k, is less than 0.100. For the cases examined in this paper the maximum Biot Number of the wall is 0.012.

coefficient ($\bar{h}_g$, $\bar{h}_a$ or $\bar{h}_L$) which is constant and/or with constant heat flux $(q/A)_w$ into the wall. Such an assumption produces an approximate result but permits its analytical treatment. Actually little is known of the nature of the coefficients of heat transfer on the inside of the vessel during discharge. It is a transient process which doubtless also involves condensation from the gas on the wall in the region of the liquid-gas interface. One result of this present study is to indicate approximate values of these coefficients from a fit with the experimental data. Numerical values of the heat transfer coefficients used to reduce the theoretical results were taken from established free convection correlations[3] and previous experimental measurements.[1]

(i) Wall Temperature Response for Heat Transfer with the Ambient

For the viewpoint of an observer fixed to the wall of the vessel the following partial differential equation derived from the first law of thermodynamics describes the transient in wall temperature owing to a transfer of heat between the wall and the ambient and the pressurizing gas and also from axial conduction in the wall itself,

$$\rho c_p \frac{\partial t}{\partial \theta} = k\left(\frac{\partial^2 t}{\partial x^2}\right) + \frac{\bar{h}_a C}{A}(t_a - t) + \frac{\bar{h}_g C}{A}(t_g - t). \qquad (1)$$

The boundary conditions on this equation are timewise variable and make its direct solution very difficult, if not impossible. An important simplification which leads to a solution can be effected, however, without compromise to the description of the physical situation, by a change in the point of observation. That is, if the observer is placed instead on the moving interface and the wall is extended to + and - infinity from an origin of coordinates at the interface, then what is described by a two-dimensional (x,θ) transient, partial differential equation, Equation (1), can be reduced to a one-dimensional (x) steady-state ordinary linear differential equation. With this configuration the liquid and gas temperature distributions remain fixed with time and it is the metal wall which flows, much like the fluid in a heat exchanger exposed to and exchanging heat simultaneously with several fluids at different temperatures along the flow path. The analytical models for this modified system are shown in Figure 2 for heat transfer with the ambient and in Figure 3 for a constant heat flux to the wall.

In the case of heat transfer with the ambient, Figure 2, two ordinary differential equations describing the wall temperature variation are derived from the first law of thermodynamics considering heat transfer between the wall and its environment and including axial heat conduction along the wall. These equations written for the liquid region ($-\infty \leq x \leq 0$) and the gas region ($0 \leq x \leq +\infty$) are as follows.

<u>$-\infty \leq x \leq 0$</u> (Liquid Region)

$$\rho c_p V \frac{dt}{dx} = k \frac{d^2t}{dx^2} + \frac{\bar{h}_a C}{A}(t_a - t) + \frac{\bar{h}_L C}{A}(t_L - t) \qquad (2)$$

<u>$0 \leq x \leq +\infty$</u> (Gas Region)

$$\rho c_p V \frac{dt}{dx} = k \frac{d^2t}{dx^2} + \frac{\bar{h}_a C}{A}(t_a - t) + \frac{\bar{h}_g C}{A}(t_g - t) \qquad (3)$$

The following boundary conditions apply. For Equation (2),

(a) at $x = 0$, $t = t^*$

(b) at $x = -\infty$, t is finite and equal to t_1

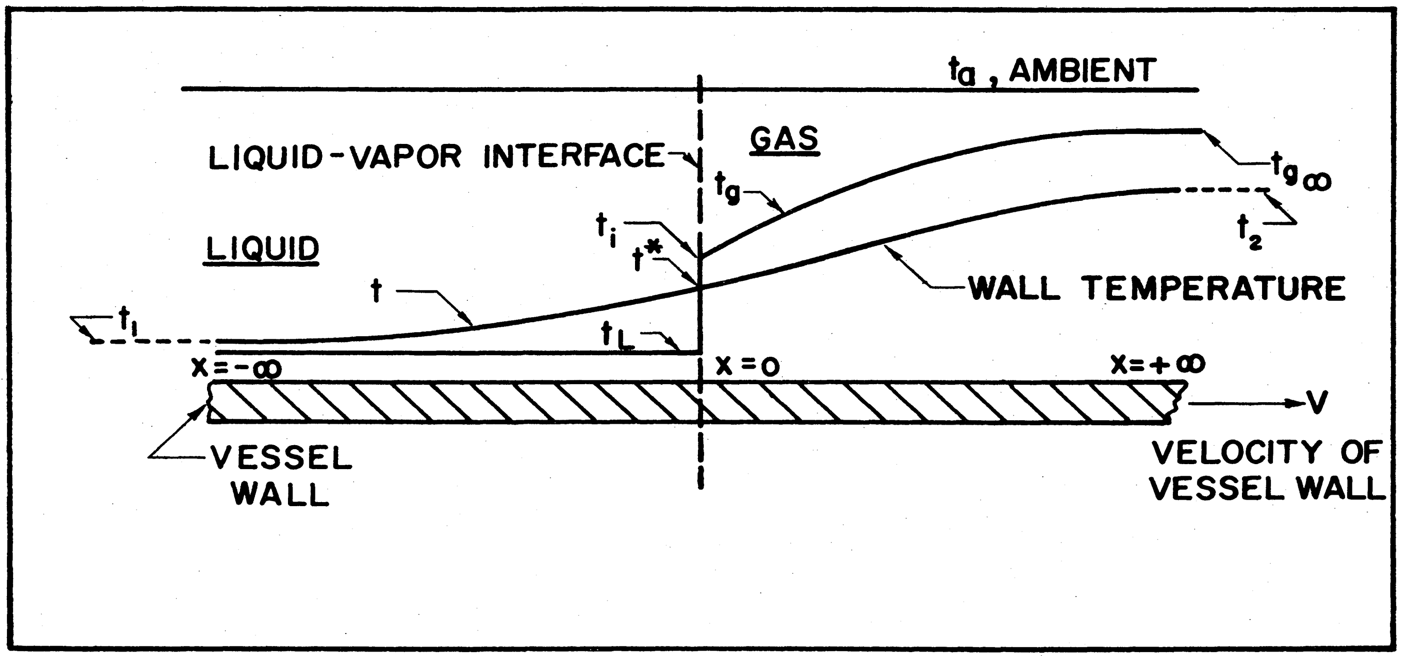

FIG. 2 MODEL FOR ANALYSIS INCLUDING HEAT TRANSFER WITH AMBIENT

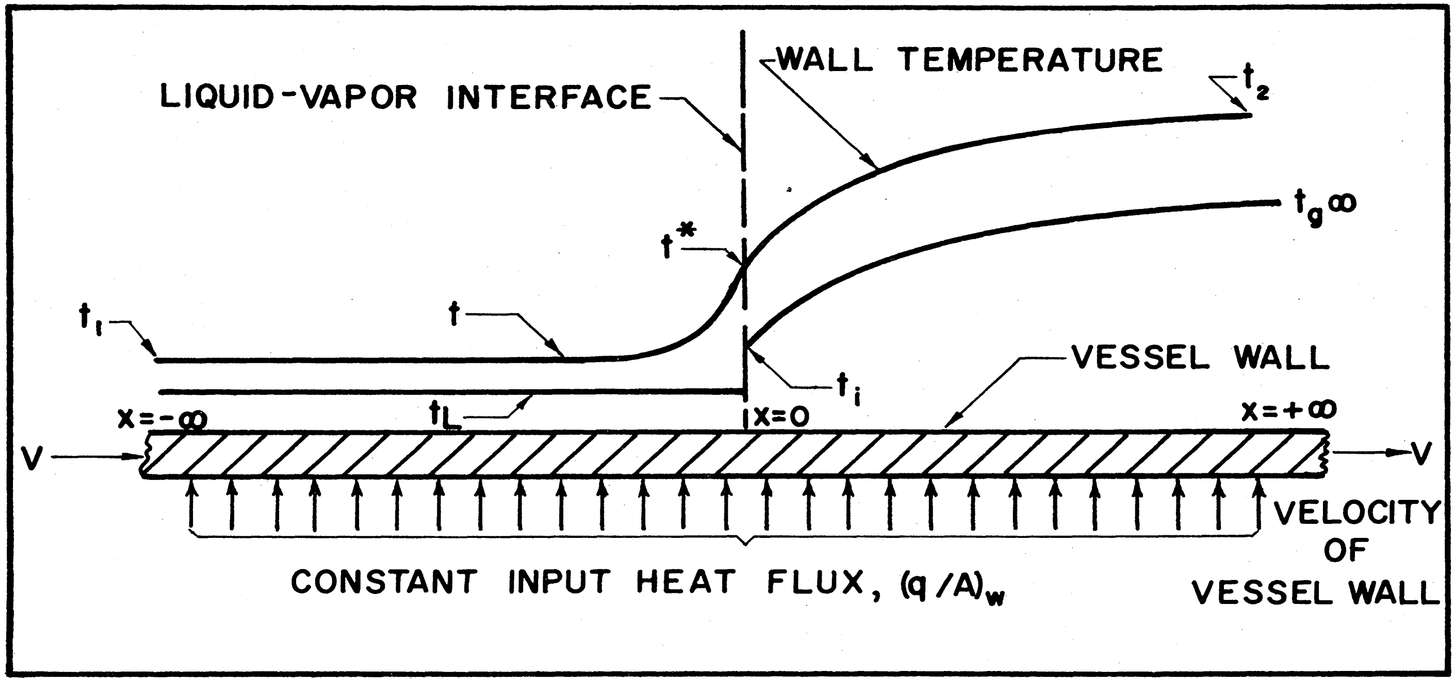

FIG. 3 MODEL FOR ANALYSIS INCLUDING CONSTANT HEAT FLUX AT WALL

For Equation (3),

(c) at $x = 0$, $t = t^*$

(d) at $x = +\infty$, t is finite and equal to t_2 .

It is necessary to make some assumptions regarding the liquid and gas temperature distributions for use in Equations (2) and (3). From experimental observations (1) it was found that during discharge the liquid remained essentially at its initial temperature except in a small region near the liquid-gas interface. At the interface the liquid and gas temperatures were that of the saturation temperature corresponding to the pressurization pressure. Further into the gas mass the temperature increased to its inlet value at the top of the vessel. Hence, it seemed reasonable to assume the liquid temperature to remain fixed at its original temperature for all values of x and to increase discontinuously to the saturation temperature at the pressurizing pressure at the liquid-gas interface as shown in Figures 2 and 3. The gas temperature was assumed to vary exponentially with x in accordance with

$$\frac{t_{g\infty} - t_g}{t_{g\infty} - t_i} = e^{-\gamma x} \quad , \tag{4}$$

which approximates its observed distribution.(1) The value of γ is selected so that at that x corresponding to the top of the vessel t_g is essentially equal to the inlet gas temperature. For purposes of analysis Equations (2) and (3) are rearranged as follows:

$$\frac{d^2t}{dx^2} - m\frac{dt}{dx} - p_1 t = - q_1 \quad (-\infty \leq x \leq 0) \tag{5}$$

and,

$$\frac{d^2t}{dx^2} - m\frac{dt}{dx} - p_2 t = Le^{-\gamma x} - q_2 \quad (0 \leq x \leq +\infty) \tag{6}$$

Equations (5) and (6) may be integrated by established methods[4] using the boundary conditions given above to obtain:

$-\infty \leq x \leq 0$ (Liquid Region)

$$t - t_1 = (t^* - t_1)e^{1/2(m + \sqrt{m^2 + 4p_1})x} \tag{7}$$

$0 \leq x \leq +\infty$) (Gas Region)

$$t - t_2 = (t^* - t_2)e^{-1/2(\sqrt{m^2 + 4p_2} - m)x} + \frac{L[e^{-\gamma x} - e^{-1/2(\sqrt{m^2 + 4p_2} - m)x}]}{\gamma^2 + m\gamma - p_2} \tag{8}$$

These results are not useful in their present form as they include the yet unspecified temperature t^*. The evaluation of t^* is accomplished by evaluating the derivative (dt/dx) at $x = 0$ from both Equations (7) and (8) and setting the results equal to each other, as is required from physical consideration. This produces the following result for t^*.

$$t^* = \frac{1}{a_1+a_2}\left[\frac{L(a_2-\gamma)}{\gamma^2+m\gamma-p_2} + a_1t_1 + a_2t_2\right], \tag{9}$$

where,

$$a_1 = 1/2(m + \sqrt{m^2 + 4p_1})$$

$$a_2 = 1/2\ (\sqrt{m^2 + 4p_2} - m)$$

$$m = \frac{\rho c_p}{k} V = \frac{V}{a}$$

$$L = \frac{\bar{h}_g C}{kA}(t_{g\infty} - t_i)$$

$$p_1 = \frac{C}{kA}(\bar{h}_a + \bar{h}_L)$$

$$p_2 = \frac{C}{kA}(\bar{h}_a + \bar{h}_g)$$

Owing to the greater value of the liquid heat transfer coefficient $\bar{h}_L$ as compared to that expected in the gas, $\bar{h}_g$, the quantity a_1 is usually very much greater than a_2. In the case considered here a_1 is about 100 times greater than a_2. Also, the first term in the brackets of Equation (9) does not contribute significantly to the value of t* over a wide range of expected values of γ. Hence it may be seen that t* is controlled primarily by t_1, as would be expected for these circumstances. In the table below a comparison is made of t* computed from Equation (9) and that obtained experimentally for runs having an inlet gas temperature of 111°F and heat transfer with an ambient at approximately 80°F.

	Case I(a)	Case II(b)
t*, Equation (9)	-305.27°F	-306.62°F
t*, Experimental (mean of 3 wall thermocouples)	-306.67°F	-306.67°F

Case I(a)	Case II(b)
$\bar{h}_a$ = 2 btu/hr - ft^2 - F	$\bar{h}_a$ = 2 btu/hr - ft^2 - F
$\bar{h}_L$ = 60 btu/hr - ft^2 - F	$\bar{h}_L$ = 60 btu/hr - ft^2 - F
$\bar{h}_g$ = 24 btu/hr - ft^2 - F	$\bar{h}_g$ = 12 btu/hr - ft^2 - F
t_L = -320°F	t_L = -320°F

These results indicate the relative insensitivity of t* to $\bar{h}_g$, the gas space heat transfer coefficient. They also suggest, however, for these pressurized-discharge processes an $\bar{h}_g$ of the order of 12 btu/hr - ft^2 - F is a more realistic value.

The axial temperature gradient in the wall at the interface may be found by differentiating Equation (7), substituting for t* from Equation (9) and evaluating at x=0, to obtain

$$\frac{dt^*}{dx} = \frac{a_1}{a_1+a_2}\left[\frac{L(a_2-\gamma)}{\gamma^2+m\gamma-p_2} - a_2(t_1 - t_2)\right] \tag{10}$$

It is of interest to examine the behavior of Equations (7), (8) and (9) when the limiting conditions of infinite and zero vessel wall velocities are imposed.* In the case of infinite wall velocity (or infinite vessel emptying speed) Equation (9) gives,

$$t^* = t_1 \tag{11}$$

Equation (8), for the region $(0 \leq x \leq +\infty)$, gives,

$$t = t^* \tag{12}$$

and, Equation (7), for the region $(-\infty \leq x \leq 0)$, gives,

$$t = t_1 \tag{13}$$

Hence, for all regions $(-\infty \leq x \leq +\infty)$ at very high liquid discharge velocities or walls having very low thermal diffusivities, or both, the wall temperature approaches t_1, that of the liquid region. This limiting condition seems reasonable on physical grounds.

At zero wall velocity (or, zero emptying speed), the wall temperature distribution in the region $(-\infty \leq x \leq 0)$ becomes:

$$t - t_1 = (t^* - t_1)e^{\sqrt{p_1}x}, \tag{14}$$

---

* From the standpoint of the thermal response of the wall it is the parameter m which governs the influence of wall velocity. This parameter is the ratio of wall or liquid-gas interface velocity to the thermal diffusivity of the wall, V/a. Large values of m correspond to large velocities or small thermal diffusivity, etc.

and for the region $(0 \leq x \leq +\infty)$ for the same condition, the wall temperature becomes,

$$t - t_2 = \left[t^* - t_1 - \frac{1}{\gamma^2 - p_2} \right] e^{-\sqrt{p_2}x} + \frac{L}{\gamma^2 - p_2} e^{-\gamma x} . \qquad (15)$$

The interface temperature t^* for use in Equations (14) and (15) is found from Equation (9) for m=0, as

$$t^* = \frac{1}{\sqrt{p_1} + \sqrt{p_2}} \left[\sqrt{p_1} t_1 + \sqrt{p_2} t_2 - \frac{L}{\gamma + \sqrt{p_2}} \right] \qquad (16)$$

For the conditions given in Case II(b) in the above table, Equation (16) predicts a limiting value of t^* equal to -288°F. Thus for the limiting conditions of $m=\infty$ and m=0, t^* falls in the fairly narrow range of about -310 to -288°F.

(ii) Wall Temperature Response for a Constant Heat Flux Input to the Wall

For the case of a constant input heat flux to the wall the differential equations describing the wall temperature variation are identical with Equations (2) and (3) except for the term $\bar{h}_a C(t_a - t)/A$, which is replaced by $(q/A)w/A$. The analytical model for this case is shown in Figure 3. The integration of the differential equations is similar to that of Equations (5) and (6). The results are as follows:

$-\infty \leq x \leq 0$ (Liquid Region)

$$t - t_1' = (t^* - t_1') e^{1/2(m + \sqrt{m^2 + 4p_L})x} \qquad (17)$$

0 $\leq$ x $\leq$ +∞) (Gas Region)

$$t - t_2' = (t^* - t_2')e^{-1/2(\sqrt{m^2 + 4p_g} - m)x}$$

$$+ \frac{L[e^{-\gamma x} - e^{-1/2(\sqrt{m^2 + 4p_g} - m)x}]}{\gamma^2 + m\gamma - p_g} \tag{18}$$

where,

$$t^* = \frac{1}{a_L + a_g}\left[\frac{L(a_g - \gamma)}{\gamma^2 + m\gamma - p_g} + a_L t_1' + a_g t_2'\right] \tag{19}$$

Comparison with Experimental Results

Comparison of the theory with experimental data both for heat transfer with the ambient to an uninsulated vessel and for a constant input heat flux is given in Figures 4, 5, 6, 7 and 8 for inlet gas temperatures from -299°F to +111°F. The ordinate, $t - t_1$, is the difference in temperature between the wall and the saturation temperature at the pressurization pressure (same as temperature of liquid-gas interface). The abcissca, X, is the difference between the thermocouple position and the instantaneous location of the liquid-gas interface. Negative values of X correspond to the liquid covering the thermocouple and positive values of X correspond to the liquid-gas interface below the thermocouple.

Figures 4, 5 and 6 are for heat transfer to the ambient and Figures 7 and 8 are for a constant input heat flux. The solid curves in all figures represent the theory and the points represent the experimental data. Thermocouples selected for this comparison are 17, 18 and 19, as shown in Figure 1. These thermocouples are far enough removed

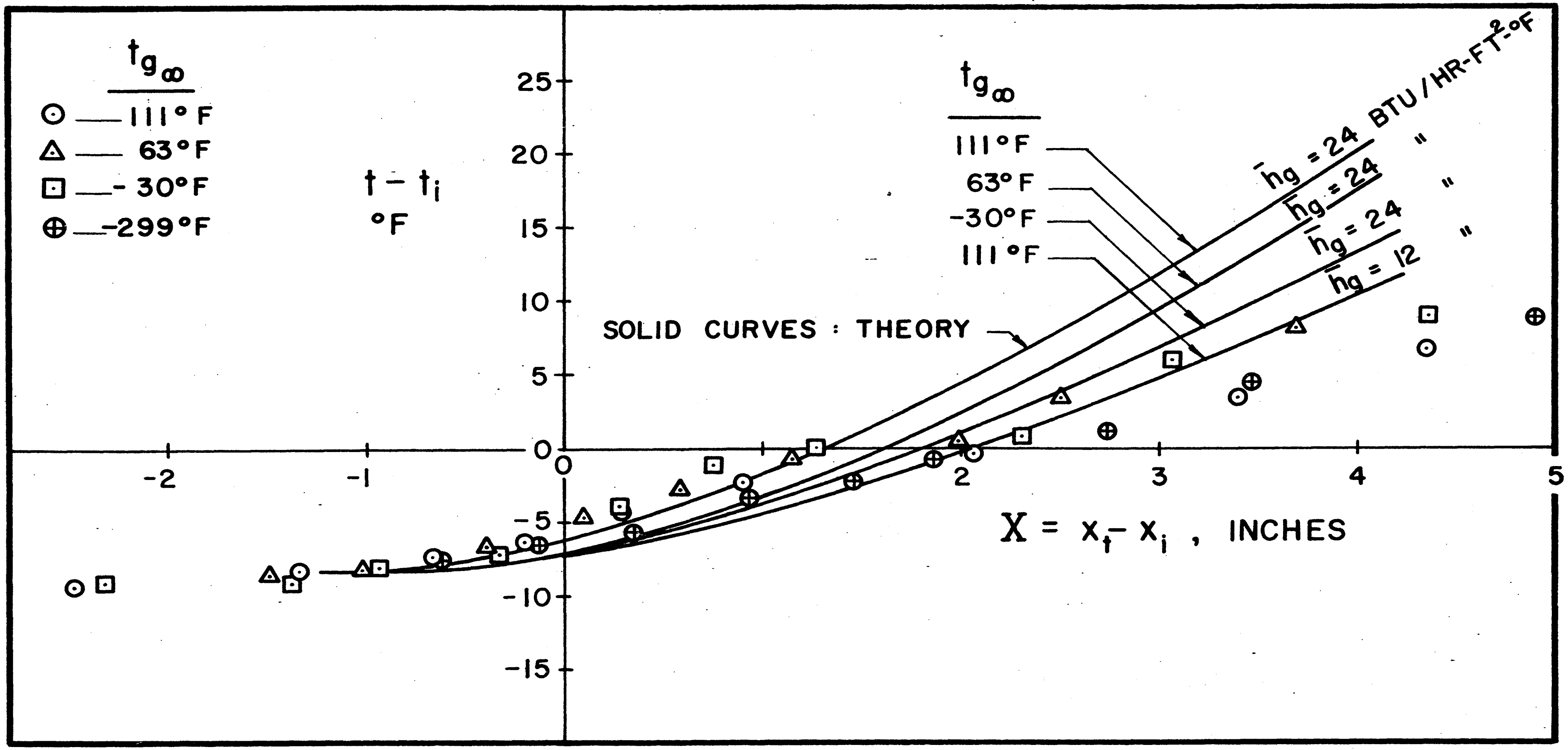

FIG. 4 WALL TEMPERATURE RESPONSE AT THERMOCOUPLE NO. 17
(INCLUDING HEAT TRANSFER WITH AMBIENT)

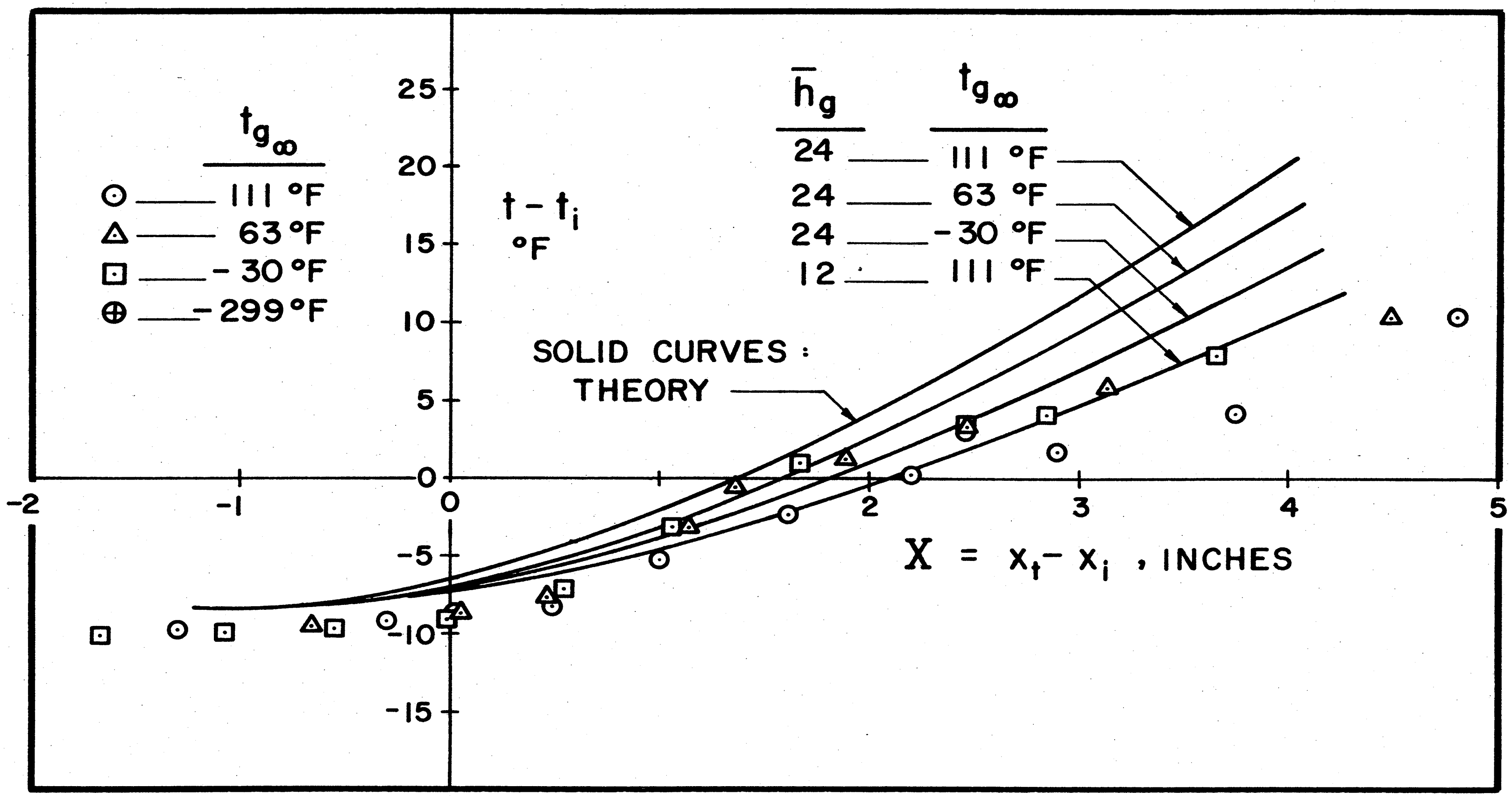

FIG. 5 WALL TEMPERATURE RESPONSE AT THERMOCOUPLE NO. 18 (INCLUDING HEAT TRANSFER WITH AMBIENT)

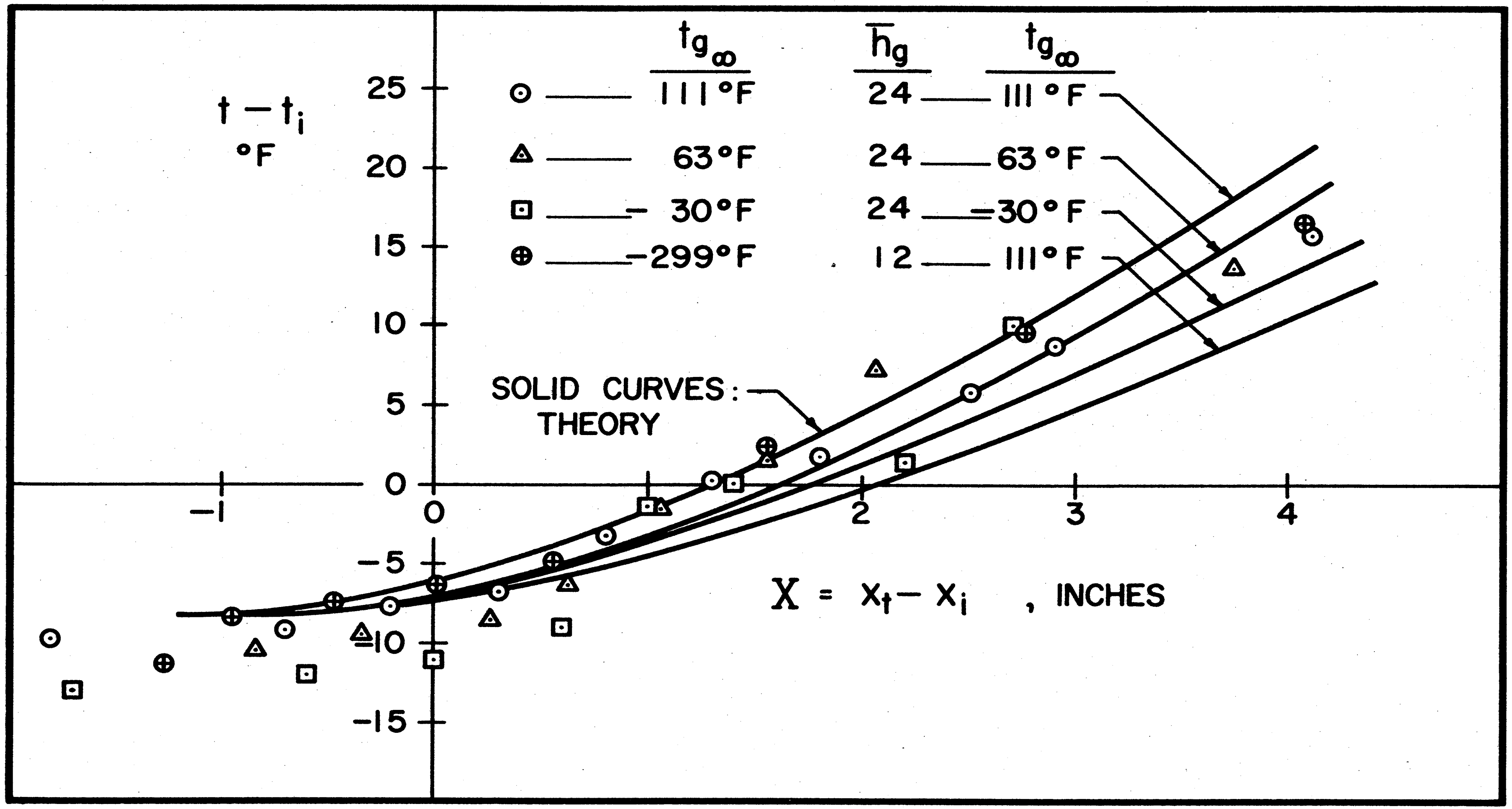

FIG — 6

WALL TEMPERATURE RESPONSE AT THERMOCOUPLE NO. 19
(INCLUDING HEAT TRANSFER WITH AMBIENT)

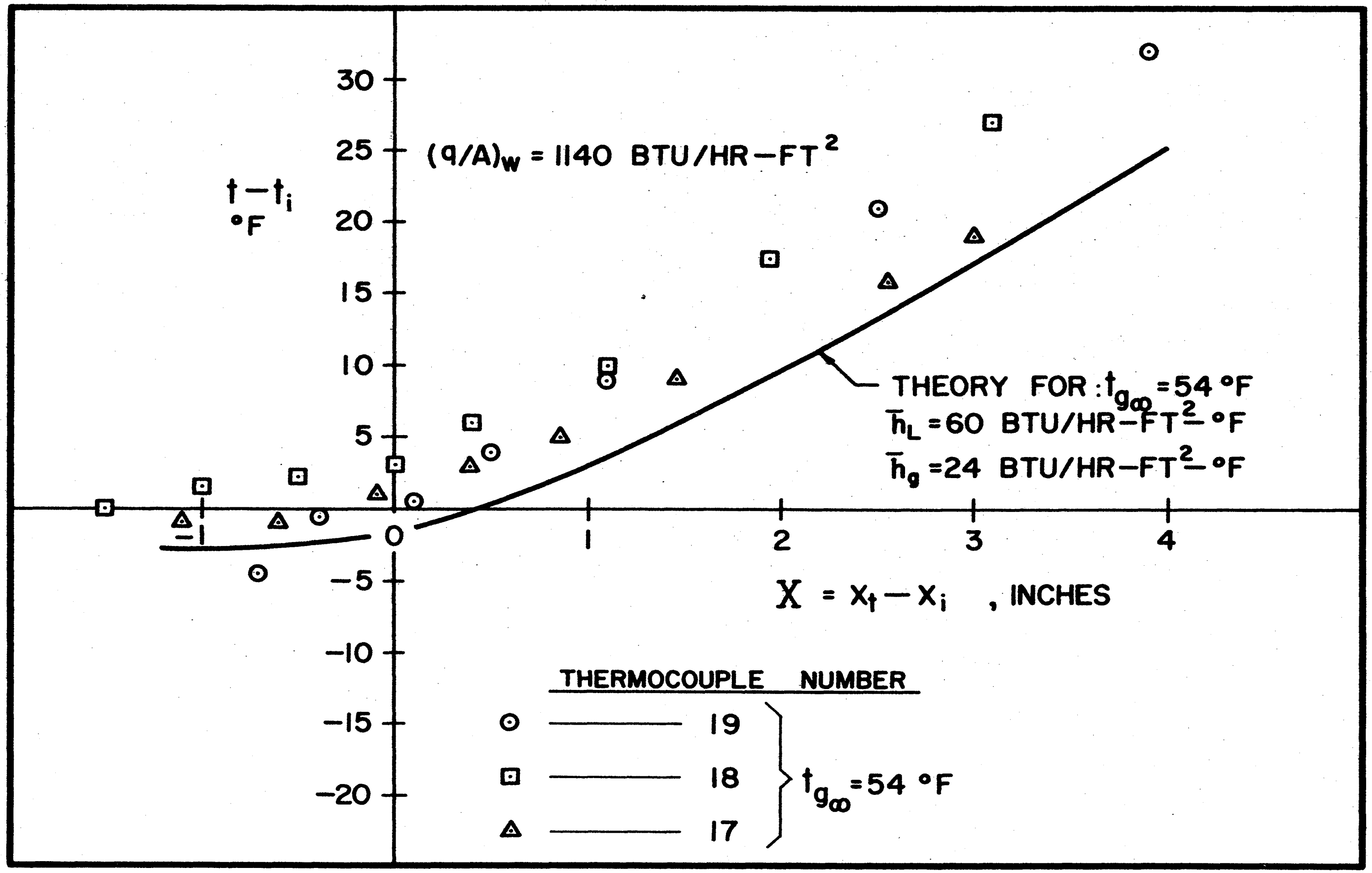

FIG — 7

WALL TEMPERATURE RESPONSE WITH WALL HEAT FLUX ESTABLISHED SIMULTANEOUSLY WITH PRESSURIZATION AND DISCHARGE

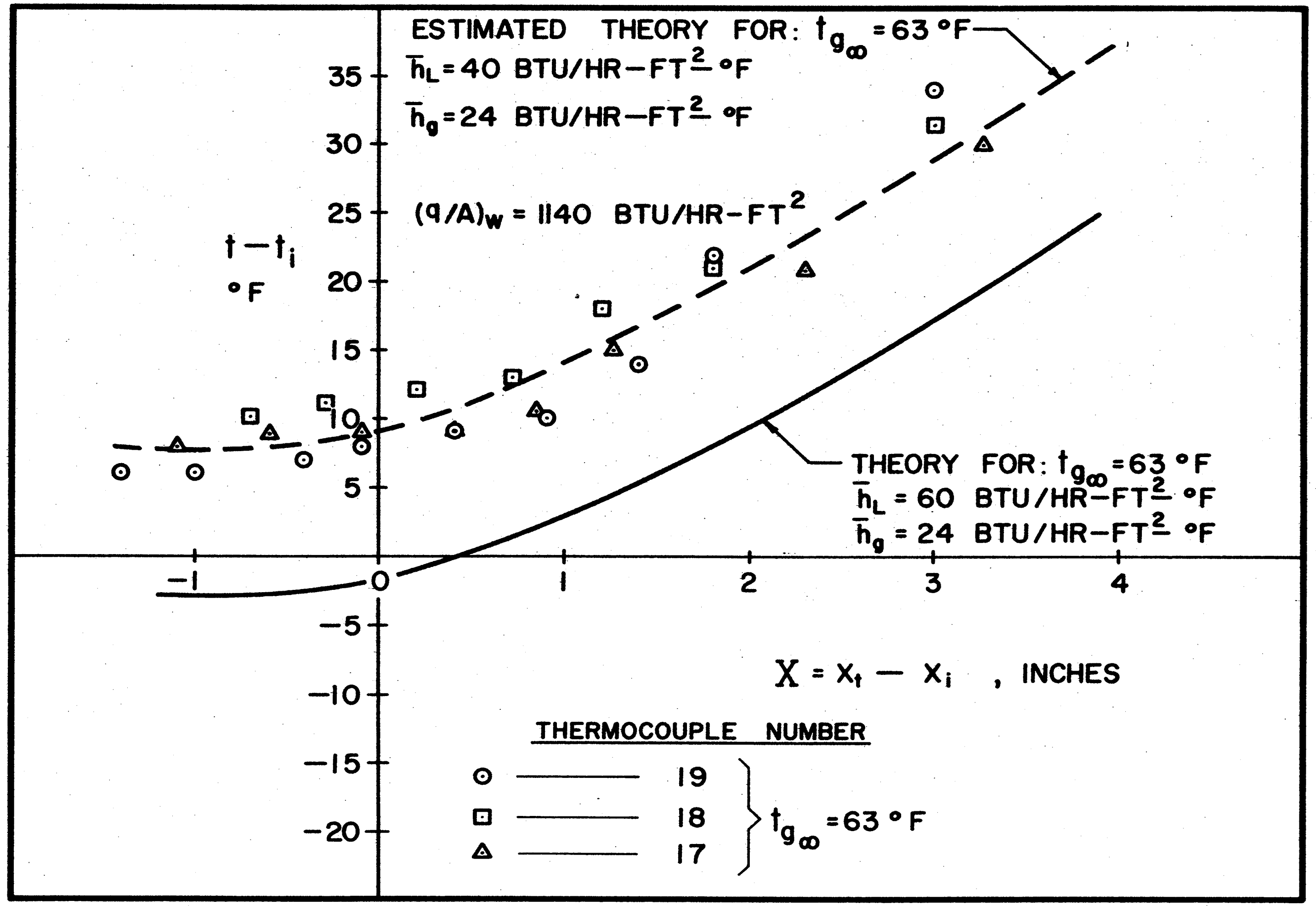

FIG–8

WALL TEMPERATURE RESPONSE WITH WALL HEAT FLUX ESTABLISHED 4 MIN. PRIOR TO PRESSURIZATION AND DISCHARGE from the ends of the vessel such that their physical behavior should reasonably well follow that of the analytical model and not appreciably be influenced by end effects. The region about each thermocouple selected for comparison with the theory includes the relative location of the thermocouple from about 2 inches below the liquid-gas interface $(X = -2)$ to about 5 inches above it $(X = 5)$.

In most cases comparison is an satisfactory as would be anticipated in view of the idealization of the analytical model and the estimated $\pm$ 1°F uncertainty in $t - t_i$ and $\pm$ 1/8 inch in X. One of the more important elements of idealization and also one of the greatest unknown parameters is the heat transfer coefficient in the gas space, $\bar{h}_g$. This was assumed to be constant in the analysis and its numerical value was taken to be 12 and 24 btu/hr - ft^2 - F. Actually it is probably not constant in time nor position but these results indicate the approximate values which predict the wall response reasonably, at least in the region of the liquid-gas interface.

An examination of the experimental points on Figures 4, 5 and 6 discloses an inflection point at small positive values of X. This is not predicted by the theory but since it was so consistently observed it is felt to be a characteristic of the system. In this range of X the wall is still subcooled with respect to t_i so it is likely the inflection point is a result of condensation on the wall from the gas. This would be followed by re-evaporation of the liquid and result in a flattening of the wall temperature profile. At larger values of X the experimental points fall below the theoretical curve except for thermocouple No. 19. This was the uppermost thermocouple so it is possible it was influenced slightly by the upper part of the vessel.

In general it appears that except in the vicinity of the liquid-gas interface a gas space heat transfer coefficient less than 12 btu/hr - ft^2 - F would fit the data better. The theory has not been worked out for other coefficients but a range from 6 to 12 btu/hr - ft^2 - F seems reasonable to provide a better fit.

The response of the wall temperature for the case of an imposed wall heat flux is given in comparison with the experimental data in Figures 7 and 8. The data of Figure 7 were taken under the conditions of simultaneous application of heat flux with pressurization and discharge. In Figure 8 the data were taken with the heat flux applied four minutes prior to pressurization and discharge, thus allowing for the establishment to an initial boiling condition.

The theoretical curves in these figures follow quite closely the general trend of the experimental points. A change in the liquid space heat transfer coefficient will bring about an improved fit. In Figure 8, for example, if $\bar{h}_L$ is reduced to 40 btu/hr - ft^2 - F, a value indicated by the experiment, a considerably better fit is obtained. The estimated curve resulting from this is shown as the dotted curve in Figure 8.

Liquid-Gas Interfacial Condensation

A problem associated with the discharge process is the heat-mass interaction of the pressurizing gas with the liquid interface. Pressurization consists of the sudden exposure of the subcooled liquid to a condensible gas at much higher temperature. This results in an immediate condensation of pressurizing gas at the interface, causing the interfacial temperature to increase suddenly to the saturation temperature corresponding to the pressurizing pressure. Two effects result: (1) a transient conduction of heat from the hotter interface to the cooler liquid, and (2) condensation of pressurizing gas on the interface. In addition there doubtless are also some convective effects in the liquid which would influence the condensation.

Assuming this interaction to be similar to that of transient heat conduction into a semi-infinite solid, estimates have been made of the temperature distributions in the liquid and the amount of pressurizing gas condensed.

Figure 9 shows the temperature of the liquid in regions below the interface at times of 1/2, 1, and 2 minutes following pressurization. The significant result of this is the predicted steep temperature gradients which exist in the liquid below the interface. That is, at the end of discharge (θ = 2 minutes), only that region of the liquid less than 1 in. below the interface has increased in temperature by more than about 4°F. At θ = 1/2 minute, only that region within 1/2 in. of the interface has increased in temperature by more than 4°F. This suggests that the bulk of the liquid is essentially uninfluenced by heat transfer with the pressurizing gas during discharge. These steep temperature gradients in the liquid have been observed [see Figure 4, Reference (1)], and have the character described in Figure 9. Furthermore, it might be expected that inlet gas temperature would have no significant effect on this process, which appears to be the case from the measurements reported.(1) The presence of these steep gradients in temperature in the liquid assist in the indication of the passage of the liquid-vapor interface from measurements of the response of the liquid thermocouples.

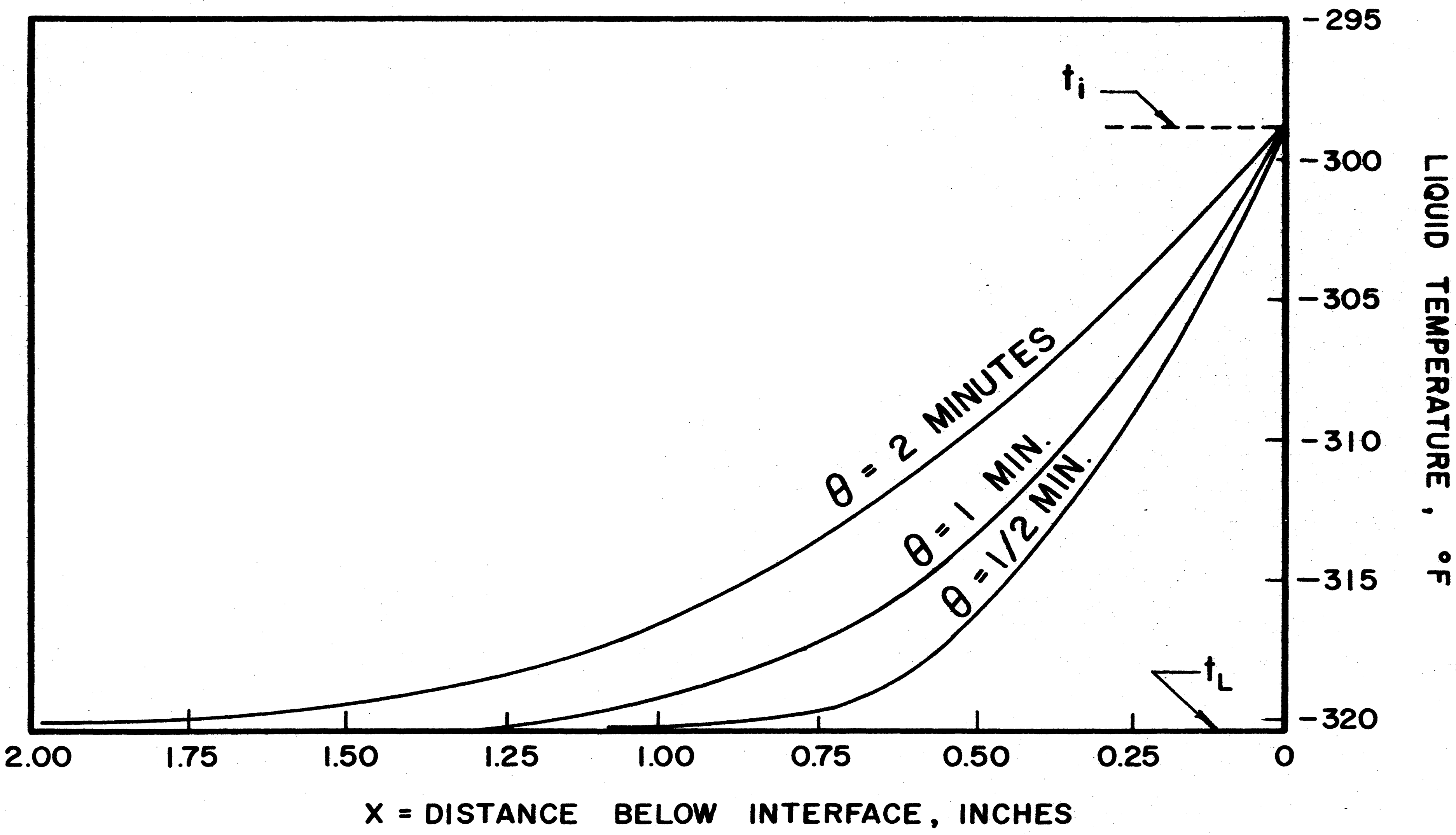

FIG. 9 LIQUID TEMPERATURE DISTRIBUTION BELOW INTERFACE

While the liquid is essentially uninfluenced by the gas, the liquid affects the gas by providing a cold surface on which the gas may condense. From the above results it is possible to estimate the amount of gas which condenses on the interface during discharge. This estimation assumes that the effect of the condensation does not alter the movement of the interface owing to a build-up of condensate. This will be reasonable if the amount of condensed gas is small, which it appears to be.

From the First Law of Thermodynamics it is seen that the heat effect of condensation, Q, at any time Θ, results in an increase of enthalpy H of the liquid. Hence,

$$\dot{Q} = mh_{fg} = \int_0^\infty (h-h_L)\, dm$$

$$= \int_0^\infty c_p \rho (t-t_L)\, A dx$$

$$= \rho\, c_p\, A(t_i-t_L) \int_0^\infty \left(\frac{t-t_L}{t_i-t_L}\right) dx \qquad (20)$$

Now, by heat-conduction theory(5):

$$\frac{t-t_L}{t_i-t_L} = 1 - \operatorname{erf} \frac{x}{2\sqrt{\alpha\Theta}} \qquad (21)$$

Thus,

$$mh_{fg} = \rho\, c_p\, A\, 2\sqrt{\alpha\Theta}\, (t_i-t_L) \int_0^\infty \left(1 - \operatorname{erf} \frac{x}{2\sqrt{\alpha\Theta}}\right) d\left(\frac{x}{2\sqrt{\alpha\Theta}}\right), \qquad (22)$$

or,

$$m = \frac{2\, \rho\, c_p\, A}{h_{fg}} \sqrt{\alpha\Theta}\, (t_i-t_L) \int_0^\infty \operatorname{erfc} \phi\, d\phi\ . \qquad (23)$$

Now, Carslaw and Jaeger,(5,p.371,373) give

$$\int_0^\infty \text{erfc}\,\phi\, d\phi = 0.564 \quad . \qquad (24)$$

Hence,

$$\frac{m}{A} = 1.128 \frac{\rho\, c_p}{h_{f_g}} (t_i - t_L) \sqrt{\alpha\theta} \qquad (25)$$

For liquid nitrogen with the following properties:

ρ = 47 lbm/ft^3

c_p = 0.49 Btu/lbm-°F

k = 0.123 Btu/hr-ft-°F

α = 0.00535

$t_i - t_L$ = 21.6°F

θ = 2 minutes

h_{f_g} = 77 Btu/lbm at 50 psia

the amount of gas condensed is about 0.10 lbm/ft^2 in 2 minutes, which is negligibly small. In 4 minutes the amount would be 0.14 lbm/ft^2 since it varies with $\theta^{1/2}$.

References

1. Van Wylen, G.J., Fenster, S.K., Merte, H., Jr., and Warren, W.A. "Pressurized-Discharge of Liquid Nitrogen from an Uninsulated Tank." Proceedings, 1958 Cryogenic Engineering Conference.

2. Fenster, S.K., Van Wylen, G.J., and Clark, J.A. "Transient Phenomena Associated with the Pressurization of Liquid Nitrogen Boiling at Constant Heat Flux." Proceedings, 1959 Cryogenic Engineering Conference.

3. McAdams, W.H. Heat Transmission. 3rd Edition, New York: McGraw-Hill Book Co., 1954.

4. Hildebrand, F.B. Advanced Calculus for Engineers. Chap. 1, New York: Prentice-Hall, Inc., 1949.

5. Carslaw, H.S. and Jaeger, J.C. Conduction of Heat in Solids. Oxford: Clarendon Press, 1950.